

Internal Report IASF-BO 406/2004

November 15, 2004

**THE INTERPLAY BETWEEN ISW EFFECT
AND LOW MULTIPOLES IN ANISOTROPIES OF CMB**

F. FINELLI¹ AND A. GRUPPUSO¹

¹*CNR-INAf/IASF, Sezione di Bologna, via P. Gobetti 101,
I-40129, Bologna, Italy*

November 15, 2004

THE INTERPLAY BETWEEN ISW EFFECT AND LOW MULTIPOLES IN ANISOTROPIES OF CMB

F. FINELLI AND A. GRUPPUSO

*CNR-INA/IASF, Sezione di Bologna, via P. Gobetti 101, I-40129, Bologna,
Italy*

SUMMARY-The Integrated Sachs-Wolfe effect is studied in order to lower the quadrupole of the anisotropies of Cosmic Microwave Background. The analysis is done for a flat Robertson-Walker metric and for a single fluid case (a unified model for dark matter and dark energy), making contact with the Λ CDM case. We show analitically that the quadrupole can be lowered down to half the value of the Λ CDM case.

1 Introduction

The low multipole of the Cosmic Microwave Background (CMB) anisotropy pattern probes the largest scales of our universe, far beyond the present Hubble radius and possibly our cosmological horizon. The measurement of this low ℓ pattern cannot be very precise since it is affected by cosmic variance, systematics (including those unexpected [1]) and foregrounds [2]. However, the two experiments so far capable to measure such low multipoles - COBE/DMR and WMAP - have detected an amplitude for the quadrupole surprisingly low compared to theoretical expectations.

Although the low amplitude for the quadrupole is not very significative at the statistical level, theoretical explanations for a low- ℓ tail should be searched. These investigations for a low quadrupole are apparently flawed by the concomitant evidence of the present acceleration of the universe. The simplest model which explains such an acceleration, i. e. Λ CDM, predicts an *increase* (compared to CDM) of the low-multipoles of the CMB spectrum due to the Integrated Sachs-Wolfe (ISW) effect, as first computed by Kofman and Starobinsky [4]. When Λ is replaced by quintessence [5], the low tail is further increased ¹.

Theoretical explanations have then been tempted in a multitude of ways. A cut-off in Fourier space has been analyzed [8, 9], finding a weak statistical evidence that this break is around the present Hubble radius. Another simple possibility is a closed universe, where there is a maximal wavelength allowed, as in a box [10]. Beyond a simple closed geometry, a low amplitude can be obtained by considering non-trivial topology [11, 12].

¹The reason for this increase is a late isocurvature effect after perturbations leave their attractor [6]

In this paper we investigate if the ISW effect can lower the quadrupole, in order to see if the conclusions reached for the Λ CDM case - an *increase* of the low tail of the CMB pattern - are generic for a Dark Energy (DE) model. We restrict ourselves to flat geometry and we analyze physical behaviour of cosmological perturbations (not in a completely phenomenological approach as in [7]). In order to make contact with the basic Λ CDM case we consider a model in which CDM and DE are described by a unique component, which mutates from dust to a component with a constant state parameter ($< -1/3$) which drives the universe into acceleration. We also assume that such component has a non-adiabatic pressure perturbation, but a vanishing speed of sound: however, we discuss the effect of relaxing such latter assumption. Our model is different from a universe filled by CDM plus DE since in that case two dynamical components are present and isocurvature perturbations are unavoidable (unless DE is described by a perfect fluid and the initial conditions are adiabatic, such as in [13, 14]).

2 The Model

In a Friedman-Robertson-Walker metric

$$ds^2 = a(\eta)^2 \left[-d\eta^2 + \frac{dr^2}{1 - Kr^2} + r^2 d\Omega^2 \right], \quad (2.1)$$

where $K = 0, \pm 1$ is the curvature of the spatial sections, Ω is the solid angle and a is the scale factor, the continuity equation for a fluid is

$$\rho' + 3\mathcal{H}(\rho + p) = 0, \quad (2.2)$$

where $\mathcal{H} = a'/a$ and η is the conformal time (related to the cosmic time by $a d\eta = dt$). We parametrize the fluid as:

$$\rho = \rho_x a^\alpha + \rho_c a^{-3}, \quad (2.3)$$

as a component which behaved as dust in the past and a component with $-\alpha/3 - 1$ as a state parameter recently. Clearly the Λ CDM behaviour is obtained for $\alpha = 0$.

We consider scalar perturbations of the metric (with $K = 0$) in the Conformal Newtonian (or Longitudinal) Gauge:

$$ds^2 = a^2(\eta) \left[-(1 + 2\psi(\eta, \vec{x}))d\eta^2 + (1 - 2\phi(\eta, \vec{x}))d\vec{x}^2 \right], \quad (2.4)$$

where $\psi(\eta, \vec{x})$ and $\phi(\eta, \vec{x})$ are the two scalar potentials. Supposing that the anisotropic stress tensor vanishes for the fluid we are considering, then $\psi(\eta, \vec{x}) = \phi(\eta, \vec{x})$.

After decoupling ($\eta > \eta_{dec}$) photons follow light-like geodesics. Because of the small deviations from the FRW metric there will be a shift in the energy for each photon. This shift does not depend on the frequency of the photon (gravity is achromatic) and it is equal to the temperature shift of a distribution of photons. The amount of the shift is given by the Sachs-Wolfe effect:

$$\frac{\Delta T}{T}(\vec{n}) = \frac{1}{3}\psi(\eta_{dec}, \vec{x}_{dec}) + 2 \int_{\eta_{dec}}^{\eta_0} d\eta \psi'(\eta, \vec{x}(\eta)), \quad (2.5)$$

where \vec{n} is the versor of the direction of the photon, η_0 is the present time, the prime (\prime) stands for derivative with respect to η , $\vec{x}(\eta) = \vec{x}_0 - (\eta_0 - \eta)\vec{n}$ (we are dealing with a spatially flat universe), $\vec{x}_{dec} = \vec{x}(\eta_{dec})$ and $\vec{x}_0 = \vec{x}(\eta_0)$. The first term is the Ordinary Sachs-Wolfe

Effect (OSWE) and it is due to the inhomogeneities of the space-time at the time of the decoupling. The second term is the Integrated Sachs-Wolfe Effect (ISWE) and it takes into account the time dependence of the gravitational field along the path of the photon.

The scale factor obeys the Friedmann equation

$$\mathcal{H}^2 = \frac{8\pi G}{3} a^2 \rho, \quad (2.6)$$

where G is the Newtonian constant and ρ is the background source, while the Fourier transform of ψ , ψ_k , satisfies

$$\psi_k'' + 3\mathcal{H}(1 + c^2)\psi_k' + [c_s^2 k^2 + 3\mathcal{H}^2(c^2 - w)]\psi_k = 0. \quad (2.7)$$

where c_s^2 and w are respectively the speed of sound and the entalpy of the source. In order to obtain such equation, the pressure perturbation of the fluid must be [15]:

$$\delta p = c_s^2 \delta \rho + 3H(1 + w) \frac{\theta \rho}{k^2} \left(c_s^2 - \frac{\dot{p}_X}{\dot{\rho}_X} \right), \quad (2.8)$$

with $c^2 = \dot{p}/\dot{\rho}$. In the following we will restrict to the case $c_s^2 \simeq 0$.

2.1 Computation of C_l

In the Fourier space Eq. (2.5) reads

$$\frac{\Delta T}{T}(\vec{n}) = \int \frac{d^3 k}{(2\pi)^3} \left[\frac{1}{3} \psi(\eta_{dec}, \vec{k}) e^{-i\vec{k} \cdot (\eta_0 - \eta_{dec}) \vec{n}} + 2 \int_{\eta_{dec}}^{\eta_0} d\eta \psi'(\eta, \vec{k}) e^{-i\vec{k} \cdot (\eta_0 - \eta) \vec{n}} \right] e^{i\vec{k} \cdot \vec{x}_0}, \quad (2.9)$$

where \vec{k} is the momentum conjugated to \vec{x} . Now it is possible to compute the two points correlation function:

$$\left\langle \frac{\Delta T}{T}(\vec{n}) \frac{\Delta T}{T}(\vec{n}') \right\rangle = \frac{1}{V} \int d^3 x_0 \frac{\Delta T}{T}(\vec{n}) \frac{\Delta T}{T}(\vec{n}'). \quad (2.10)$$

Notice that $\langle \dots \rangle$ means average over the positions of observation. Replacing Eq. (2.9) in Eq. (2.10) one obtains

$$\begin{aligned} \left\langle \frac{\Delta T}{T}(\vec{n}) \frac{\Delta T}{T}(\vec{n}') \right\rangle = \int \frac{d^3 k}{(2\pi)^3} & \left[\frac{1}{3} \psi(\eta_{dec}, \vec{k}) e^{-i\vec{k} \cdot (\eta_0 - \eta_{dec}) \vec{n}} + 2 \int_{\eta_{dec}}^{\eta_0} d\eta \psi'(\eta, \vec{k}) e^{-i\vec{k} \cdot (\eta_0 - \eta) \vec{n}} \right] \\ & \left[\frac{1}{3} \psi(\eta_{dec}, \vec{k}) e^{-i\vec{k} \cdot (\eta_0 - \eta_{dec}) \vec{n}'} + 2 \int_{\eta_{dec}}^{\eta_0} d\eta \psi'(\eta, \vec{k}) e^{-i\vec{k} \cdot (\eta_0 - \eta) \vec{n}'} \right]^* \end{aligned} \quad (2.11)$$

where $*$ stands for complex conjugation. Using now the following relation

$$e^{-i\vec{k} \cdot (\eta_0 - \eta) \vec{n}} = \sum_{l=0}^{\infty} (2l+1) j_l(k(\eta_0 - \eta_{dec})) P_l(\hat{k} \cdot \vec{n}), \quad (2.12)$$

where $\hat{k} = \vec{k}/|\vec{k}|$, j_l are the spherical Bessel functions and P_l are the Legendre polynomials, and considering that

$$P_l(\hat{k} \cdot \vec{n}) = \frac{4\pi}{(2l+1)} \sum_m Y_{lm}^*(\hat{k}) Y_{lm}(\vec{n}), \quad (2.13)$$

where Y_{lm} are the spherical harmonics, and once splitted the integration $d^3 k = k^2 dk d\Omega_k$, using the following orthonormality relation

$$\int d\Omega_k Y_{lm}^*(\hat{k}) Y_{l'm'}(\hat{k}) = \delta_{ll'} \delta_{mm'}, \quad (2.14)$$

one obtains

$$\langle \frac{\Delta T}{T}(\vec{n}) \frac{\Delta T}{T}(\vec{n}') \rangle = \sum_{l=0}^{\infty} \frac{(2l+1)}{4\pi} P_l(\vec{n} \cdot \vec{n}') C_l, \quad (2.15)$$

where

$$C_l = \frac{2}{\pi} \int_0^{\infty} dk k^2 \left[\frac{1}{3} \psi(\eta_{dec}, \vec{k}) j_l(k(\eta_0 - \eta_{dec})) + 2 \int_{\eta_{dec}}^{\eta_0} d\eta \psi'(\eta, \vec{k}) j_l(k(\eta_0 - \eta)) \right]^2. \quad (2.16)$$

The function given in Eq. (2.16) (which is called CMB power spectrum) represents the amount of fluctuation at the scale l . At the time of decoupling ($\eta = \eta_{dec}$) the power spectrum of the metric perturbation is written as $P_k = k^3 |\psi_k(\eta_{dec})|^2 = \bar{A}^2(\eta_0 k)^{n_s-1} f^2(\eta_{dec})/4$, and in the limit of small k (i.e. large scales limit) it is possible to write $\psi_k(\eta) = \psi_k f(\eta)$ where ψ_k is tuned at the time of decoupling ($\psi_k = \bar{A}(\eta_0 k)^{(n_s-4)/2}/2$) and $f(\eta)$ is given by

$$f(\eta) = 1 - \frac{a'}{a^3} \int_0^{\eta} d\tau a^2(\tau), \quad (2.17)$$

that is the Kofman-Starobinski solution [4]. Then replacing in Eq. (2.16) one gets the following expression for C_l :

$$C_l = \frac{2\bar{A}^2 \eta_0^{n_s-1}}{\pi} \int_0^{k^*} \frac{dk}{k^{(2-n_s)}} \left[\frac{1}{10} j_l(k \eta_0) + \int_0^{\eta_0} d\eta f'(\eta) j_l(k(\eta_0 - \eta)) \right]^2, \quad (2.18)$$

where it has been chosen $\eta_{dec} = 0$, $f(\eta_{dec} = 0) = 3/5$; k^* is a cut off due to the approximated solution of Eq. (2.17) and n_s is the spectral index ($n_s = 1$ when the spectrum is scale invariant). When $c_s^2 = 0$ (see Eq. (2.7)), as in the Λ CDM model or in the model we are considering ², the solution (2.17) is exact and there is no need of a cut-off (i.e. $k^* = \infty$).

2.2 Analytical Computation

Replacing eq. (2.3) in eq. (2.6), it is possible to integrate for η :

$$\eta(a) = \frac{2}{\mathcal{H}_0} \left(\frac{a}{\Omega_{c0}} \right)^{1/2} {}_2F_1 \left[\frac{1}{6+2\alpha}, \frac{1}{2}, 1 + \frac{1}{6+2\alpha}, -a^{3+\alpha} \frac{\Omega_{x0}}{\Omega_{c0}} \right], \quad (2.19)$$

where ${}_2F_1$ is an Hypergeometric Function, $\Omega_i = \rho_i/\bar{\rho}$ with $\bar{\rho} = 3\mathcal{H}/(8\pi G a^2)$ and in general the subscript $_0$ means that the function which the label is appended to, has to be computed at the present (conformal) time. Notice that

$$\frac{\Omega_{x0}}{\Omega_{c0}} = \frac{\rho_x}{\rho_c}, \quad (2.20)$$

and moreover remember that from eq. (2.6) we have

$$\Omega_{x0} + \Omega_{c0} = 1. \quad (2.21)$$

In order to compute C_l (see eq. (2.18)), one has to take the time derivative of eq. (2.17) and using also eq. (2.6), one gets

$$f'(a) = a \sqrt{\frac{8\pi G}{3}} \left[\frac{2}{5} \left(\rho_x a^\alpha \left(1 - \frac{\alpha}{2}\right) + \frac{5}{2} \rho_c a^{-3} \right) \sqrt{\frac{a^3}{\rho_c}} F(a) - \left(\rho_x a^\alpha + \rho_c a^{-3} \right)^{1/2} \right], \quad (2.22)$$

²See Section 2.

where

$$F(a) = {}_2F_1 \left[\frac{5}{6+2\alpha}, \frac{1}{2}, 1 + \frac{5}{6+2\alpha}, -a^{3+\alpha} \frac{\Omega_{x0}}{\Omega_{c0}} \right] \quad (2.23)$$

Since in general eq. (2.19) is not invertible³, it is not possible to have (analytically) f' as a function of η . In order to have an analytical expression for the ISWE (see eq. (2.18)), it is necessary to change the variable of integration from η to a :

$$C_l = \frac{2\bar{A}\eta_0^{n_s-1}}{\pi} \int_0^{k^*} \frac{dk}{k^{(2-n_s)}} \left[\frac{1}{10} j_l(k\eta(1)) + \int_0^1 da \frac{df}{da} j_l(k(\eta(1) - \eta(a))) \right]^2, \quad (2.24)$$

with $a(\eta_0) = 1$ and where:

$$\frac{df}{da} = \frac{1}{a} \left[\frac{\frac{2}{5}(1 - \frac{\alpha}{2}) \frac{\rho_x}{\rho_c} a^{\alpha+3} + 1}{\left(\frac{\rho_x}{\rho_c} a^{\alpha+3} + 1 \right)^{1/2}} F(a) - 1 \right]. \quad (2.25)$$

It is interesting to notice that in the following limit (i.e. $(\rho_x/\rho_c)a^{\alpha+3} \ll 1$, $0 < a < 1$), $df/da \rightarrow 0$. This confirms a known result: when the evolution of a is power law like (as in the case of CDM source) then ISWE vanishes.

Because of numerical analysis, it is better to deal with dimensionless variables. Then it is useful to rescale the variable k as follows $s = k/\mathcal{H}_0$. One obtains:

$$C_l = \frac{2\bar{A}(\eta_0\mathcal{H}_0)^{n_s-1}}{\pi} \int_0^{s^*} \frac{ds}{s^{(2-n_s)}} \left[\frac{1}{10} j_l(s\chi(1)) + \int_0^1 da \frac{df}{da} j_l(s(\chi(1) - \chi(a))) \right]^2, \quad (2.26)$$

where $s^* = k^*/\mathcal{H}_0$ and $\chi(a) = \mathcal{H}_0 \eta(a)$.

3 Numerical Results

We consider the scale invariant case ($n_s = 1$) and as already announced, we take into account a source such that its pressure does not depend on ρ (then $s^* = \infty$):

$$C_l = \frac{2\bar{A}}{\pi} \int_0^\infty \frac{ds}{s} \left[\frac{1}{10} j_l(s\chi(1)) + \int_0^1 da \frac{df}{da} j_l(s(\chi(1) - \chi(a))) \right]^2. \quad (3.1)$$

We focus on the quadrupole (i.e. $l = 2$). The numerical results are organized in Table I. The integration is obtained starting from $s = 1/5$ and stopping at $s = 25$. These cut-offs are chosen in such a way that the numbers put in the table are stable if the range of integration is made wider. The first observation deal with the qualitative lowering of the quadrupole:

³For $\alpha = 0$ (i.e. Λ CDM model) it is invertible [4], but one has to make the computation in the cosmic time t and not in the conformal time η .

Ω_{x0}	Ω_{c0}	$\alpha = -2$	$\alpha = -1$	$\alpha = 0$	$\alpha = 1$	$\alpha = 2$	$\alpha = 3$	$\alpha = 4$
1/10	9/10	0.00080	0.00081	0.00082	0.00082	0.00083	0.00083	0.00083
7/10	3/10	0.00066	0.00092	0.00115	0.00133	0.00147	0.00156	0.00161
9/10	1/10	0.00058	0.00131	0.00219	0.00304	0.00380	0.00444	0.00494

Table 1: $C_2\pi/2\bar{A}$ vs α and Ω_{x0}, Ω_{c0} .

it exists if α is negative. Second, we notice that such a lowering is quantitatively bigger if Ω_{x0}/Ω_{c0} is larger and larger. This is understandable since this is the regime in which the ISWE is important (in the opposite regime ISWE tends to zero). As instance, in the most interesting case (i.e. $\Omega_{x0} = 7/10$ and $\Omega_{c0} = 3/10$), we get a lowering of the 42 % for $\alpha = -2$ with respect to $\alpha = 0$.

In order to understand the behaviour described in the first observation, we rewrite eq. (3.1) in the following way:

$$\frac{C_{l\pi}}{2A} = \int_0^\infty ds [F_1(s) + F_2(s) + F_3(s)] , \quad (3.2)$$

where

$$F_1(s) = \frac{1}{100s} j_2(s\chi(1))^2 , \quad (3.3)$$

$$F_2(s) = \left[\int_0^1 da \frac{df}{da} j_2(s(\chi(1) - \chi(a))) \right]^2 / s , \quad (3.4)$$

$$F_3(s) = \frac{1}{5s} j_2(s\chi(1)) \left[\int_0^1 da \frac{df}{da} j_2(s(\chi(1) - \chi(a))) \right] , \quad (3.5)$$

and we plot these three functions for different values of α (See Fig. 1, 2, 3). Ω_{x0} and Ω_{c0} are fixed respectively to 7/10 and 3/10. We used different colors in order to distinguish among the values of α : Black corresponds to $\alpha = -2$, Blu to $\alpha = -1$, Red to $\alpha = 0$, Green to $\alpha = 1$, Sky Blu to $\alpha = 2$.

It is clear that we have to look at the areas subtended by these curves and sum up the three contributions in order to obtain the quadrupole. Here there are some observations:

- We checked that the areas under the curves of Fig. 1 is always the same and it is equal to 0.00083. The dependence on α appears in next digit.
- The area subtended by the curves in Fig. 2 is the smallest for $\alpha = -2$ and it becomes bigger and bigger for increasing α .
- The mixing term (Fig. 3 gives a negative contribution that is the biggest (in absolute value) for $\alpha = -2$ and it becomes smaller and smaller (in absolute value) for increasing α .

4 Conclusion

In this paper we have computed the quadrupole of the CMB anisotropies for a fluid which behaved dust in the past, but capable to drive the universe into acceleration recently. We have approximated the state parameter of this fluid as constant and we have neglected baryons in our analysis. By requiring a vanishing speed of sound for this component (as for CDM in standard cosmology) we have computed semianalytically the quadrupole of the CMB temperature pattern and we have demonstrated that it can be lowered approximatively to half of the Λ CDM value.

A Appendix: The Generalized Chaplygin Gas

In this appendix we repeat the same calculation for another model which has shown a decrease in the amplitude of the low- ℓ pattern of CMB temperature anisotropies, namely the Generalized Chaplygin Gas studied in [13, 14].

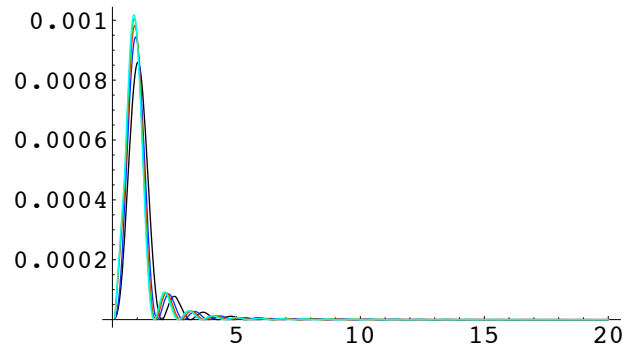


Figure 1: $F_1(s)$: Integrand of the Ordinary Sachs-Wolfe effect for different values of α .

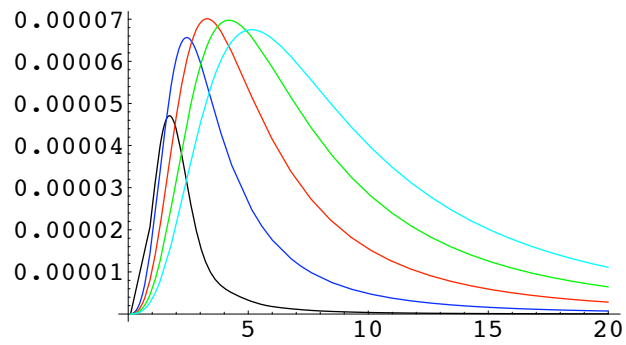


Figure 2: $F_2(s)$: Integrand of Integrated Sachs-Wolfe effect for different values of α .

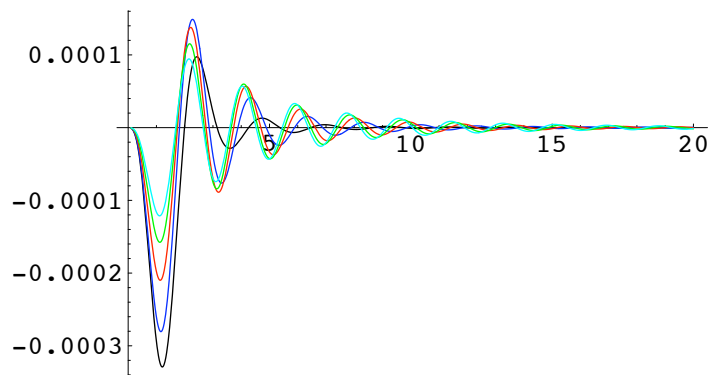


Figure 3: $F_3(s)$: Integrand of the the mixing term for different values of α .

A.1 Some features of this gas

The GCG is characterized by the following equation of state:

$$p_X = -\frac{A}{\rho_X^\beta}, \quad (\text{A.1})$$

where p_X is the pressure and ρ_X is the energy density of the GCG, β and B are two free positive parameters ($\beta = 1$ corresponds to Chaplygin Gas). In this case ρ_X can be exactly integrated

$$\rho_X = \left(A + \frac{B}{a^{3(1+\beta)}} \right)^{1/(1+\beta)}, \quad (\text{A.2})$$

where A and B are constants of dimensions $M^{4(1+\beta)}$. If $\beta = 0$ then GCG recovers Λ CDM model (i.e. CDM model with a Cosmological Constant), while if $B = 0$ then GCG recovers CDM model.

From eq. (A.2) it is clear that GCG behaves like dust when $B/A \gg a^{3(1+\beta)}$ (assuming $a = 1$ at the present time) while it behaves like a cosmological constant in the opposite regime ($B/A \ll a^{3(1+\beta)}$). This explains why the GCG is an unified model for CDM and DE.

Moreover in the limit of large a it is possible to show that GCG is the sum of a cosmological constant and a subdominant perfect fluid with equation of state $p = \beta\rho$. This allows for a physical interpretation of the parameter β .

The entalpy w_X is given by

$$w_X = \frac{p_X}{\rho_X} = -\frac{A}{\rho_X^{1+\beta}} = -\frac{A}{A + \frac{B}{a^{3(1+\beta)}}}, \quad (\text{A.3})$$

and decreases from 0 (corresponding to $a = 0$) to -1 ($a = \infty$).

The speed of sound c_X^2 for the GCG is given by ⁴

$$c_X^2 = \frac{\partial p_X}{\partial \rho_X} = \beta \frac{A}{\rho_X^{1+\beta}} = -\beta w_X, \quad (\text{A.4})$$

then it takes values from 0 (corresponding to $a = 0$) to β (corresponding to $a = \infty$). In order to have a speed of sound at most luminal we set $0 \leq \beta \leq 1$.

A.2 Analytical Computation for the GCG

Replacing eq. (A.2) in eq. (2.6), it is possible to integrate for η :

$$\eta(a) = \frac{2}{\mathcal{H}_0} \left(1 + \frac{A}{B}\right)^{\frac{1}{2(1+\beta)}} a^{1/2} {}_2F_1 \left[\frac{1}{6(1+\beta)}, \frac{1}{2(1+\beta)}, 1 + \frac{1}{6(1+\beta)}, -a^{3(1+\beta)} \frac{A}{B} \right], \quad (\text{A.1})$$

where ${}_2F_1$ is an Hypergeometric Function and \mathcal{H}_0 is the value of the Hubble rate at the present (conformal) time.

In order to compute C_l (see eq. (2.18)), one has to take the time derivative of eq. (2.17) and using also eq. (2.6), one gets

$$f'(a) = \frac{1}{\sqrt{3}M_{Pl}} \left[\frac{2}{5} \frac{A + \frac{5}{2}Ba^{-3(1+\beta)}}{\left(A + \frac{B}{a^{3(1+\beta)}}\right)^{\beta/(1+\beta)}} \frac{a^{5/2}}{B^{1/(2(1+\beta))}} G(a) - a \left(A + \frac{B}{a^{3(1+\beta)}} \right)^{1/(2(1+\beta))} \right] \quad (\text{A.2})$$

⁴Notice that since p_X depends on time only through ρ_X (see eq. (A.1)), the two definitions for the speed of sound, given in Section 2, coincide.

	$\alpha = 0$	$\alpha = 1/10$	$\alpha = 1/4$	$\alpha = 1/2$	$\alpha = 1$	$\alpha = 2$
$A/B = 1$	0.00082	0.00082	0.00082	0.00081	0.00081	0.00081
$A/B = 7/3$	0.00096	0.00092	0.00089	0.00086	0.00083	0.00081
$A/B = 10$	0.00195	0.00180	0.00160	0.00134	0.00104	0.00085

Table 2: $C_2\pi/(2\bar{A})$ vs β and A/B with $UV = 6$ and $IR = 1/5$ where $n_s = 1$.

where

$$G(a) = {}_2F_1 \left[\frac{5}{6(1+\beta)}, \frac{1}{2(1+\beta)}, 1 + \frac{5}{6(1+\beta)}, -a^{3(1+\beta)} \frac{A}{B} \right].$$

Since in general eq. (A.1) is not invertible⁵, it is not possible to have (analytically) f' as a function of η . In order to have an analytical expression for the ISWE (see eq. (2.18)), it is necessary to change the variable of integration from η to a :

$$C_l = \frac{2\bar{A}\eta_0^{n_s-1}}{\pi} \int_0^{k^*} \frac{dk}{k^{(2-n_s)}} \left[\frac{1}{10} j_l(k\eta(1)) + \int_0^1 da \frac{df}{da} j_l(k(\eta(1) - \eta(a))) \right]^2, \quad (\text{A.3})$$

with $a(\eta_0) = 1$ and where:

$$\frac{df}{da} = \frac{1}{a} \left[\frac{2}{5} \frac{1 + \frac{5}{2} B/A a^{-3(1+\beta)}}{\left(1 + \frac{B/A}{a^{3(1+\beta)}}\right)^{(\beta+1/2)/(1+\beta)}} \left(\frac{B/A}{a^{3(1+\beta)}}\right)^{-1/(2(\beta+1))} G(a) - 1 \right]. \quad (\text{A.4})$$

It is interesting to notice that in the dust limit (i.e. $B/A \gg a^{3(1+\beta)}$, $0 < a < 1$, $\beta > 0$), $df/da \rightarrow 0$. This confirms a known result: when the evolution of a is power law like (as in the case of CDM source) then ISWE vanishes.

Because of numerical analysis, it is better to deal with dimensionless variables. Then it is useful to rescale the variable k as follows $s = k/\mathcal{H}_0$. One obtains:

$$C_l = \frac{2\bar{A}(\eta_0\mathcal{H}_0)^{n_s-1}}{\pi} \int_0^{s^*} \frac{ds}{s^{(2-n_s)}} \left[\frac{1}{10} j_l(s\chi(1)) + \int_0^1 da \frac{df}{da} j_l(s(\chi(1) - \chi(a))) \right]^2, \quad (\text{A.5})$$

where $s^* = k^*/\mathcal{H}_0$ and $\chi(a) = \mathcal{H}_0 \eta(a)$.

A.3 Numerical Results for GCG

Again we consider the scale invariant case, so we set $n_s = 1$ in eq. (A.5). See table 2.

References

- [1] A. Gruppuso, C. Burigana, F. Finelli, Internal Report IASF-BO 405/2004 (2004).
- [2] L. R. Abramo and L. Sodre Jr., astro-ph/0312124.
- [3] G. Efstathiou, 2003, MNRAS, 346, L26.
- [4] L. Kofman, A.A. Starobinsky, Pisma Astron. Zh. 11, 643 (1985) [Sov. Astron. Lett. 11, 271 (1985)]

⁵For $\beta = 0$ (i.e. Λ CDM model) it is invertible and one gets the Kofman-Starobinski solution [4]. But to see this, it is necessary to work in the proper time t .

- [5] B. Ratra and P.J.E. Peebles, 1998, Phys. Rev. D 37, 3406; C. Wetterich, 1998, Nucl. Phys. B, 302, 645; J. Frieman, C. Hill, A. Stebbins and I. Waga, PRL, 75, 2077 (1995); R.R. Caldwell, R. Dave, P.J. Steinhardt, 1995, PRL, 75, 2077.
- [6] L. R. Abramo and F. Finelli, 2001, Phys. Rev. D 64, 083513.
- [7] T. Multamaki and O. Elgaroy, A & A 423, 811 (2004) astro-ph/0312534.
- [8] S.L. Bridle, A.M. Lewis, J. Weller, G. Efstathiou, 2003, MNRAS, 342, L72
- [9] C.R. Contaldi, M. Peloso, L. Kofman, A. Linde, 2003, JCAP, 0307, 002.
- [10] G. Efstathiou, 2003, MNRAS, 343, L95.
- [11] J.-P. Luminet, J. Weeks, A. Riazuelo, R. Lehoucq, J.-P. Uzan, 2003, Nature 425, 593.
- [12] N. J. Cornish, D. N. Spergel, G. D. Starkman, E. Komatsu, Phys. Rev. Lett. 92, 201302 (2004).
- [13] D. Carturan, F. Finelli, Phys.Rev.D68:103501,2003
- [14] L. Amendola, F. Finelli, C. Burigana, D. Carturan, JCAP 0307:005,2003.
- [15] L.R. Abramo, F. Finelli, T.S. Pereira, Phys. Rev. **D 70** 063517 (2004).